Instrument Science Report ACS 2016-06

Here Be Dragons: Characterization of ACS/WFC Scattered Light Anomalies

Blair Porterfield, Dan Coe, Shireen Gonzaga, Jay Anderson, Norman Grogin

November 1, 2016

Abstract

We present a study characterizing scattered light anomalies that occur near the edges of Advanced Camera for Surveys (ACS) Wide Field Channel (WFC) images. We inspected all 8,573 full-frame ACS/WFC raw images with exposure times longer than 350 seconds obtained in the F606W and F814W filters from 2002 to October 2013. We visually identified two particular scattered light artifacts known as "dragon's breath" and edge glow. Using the 2MASS point source catalog and Hubble Guide Star Catalog (GSC II), we identified the stars that caused these artifacts. The stars are all located in narrow bands ($\sim 3''$ *across) just outside the ACS/WFC field of view (*$2'' - 16''$ *away). We provide a map of these risky areas around the ACS/WFC detectors – users should avoid positioning bright stars in these regions when designing ACS/WFC imaging observations. We also provide interactive webpages which display all the image artifacts we identified, allowing users to see examples of the severity of artifacts they might expect for a given stellar magnitude at a given position relative to the ACS/WFC field of view. On average, 10th (18th) magnitude stars produce artifacts about 1,000 (100) pixels long. But the severity of these artifacts can vary strongly with small positional shifts (*$\sim 1''$*). The results are similar for both filters (F606W and F814W) when expressed in total fluence, or flux multiplied by exposure time.*

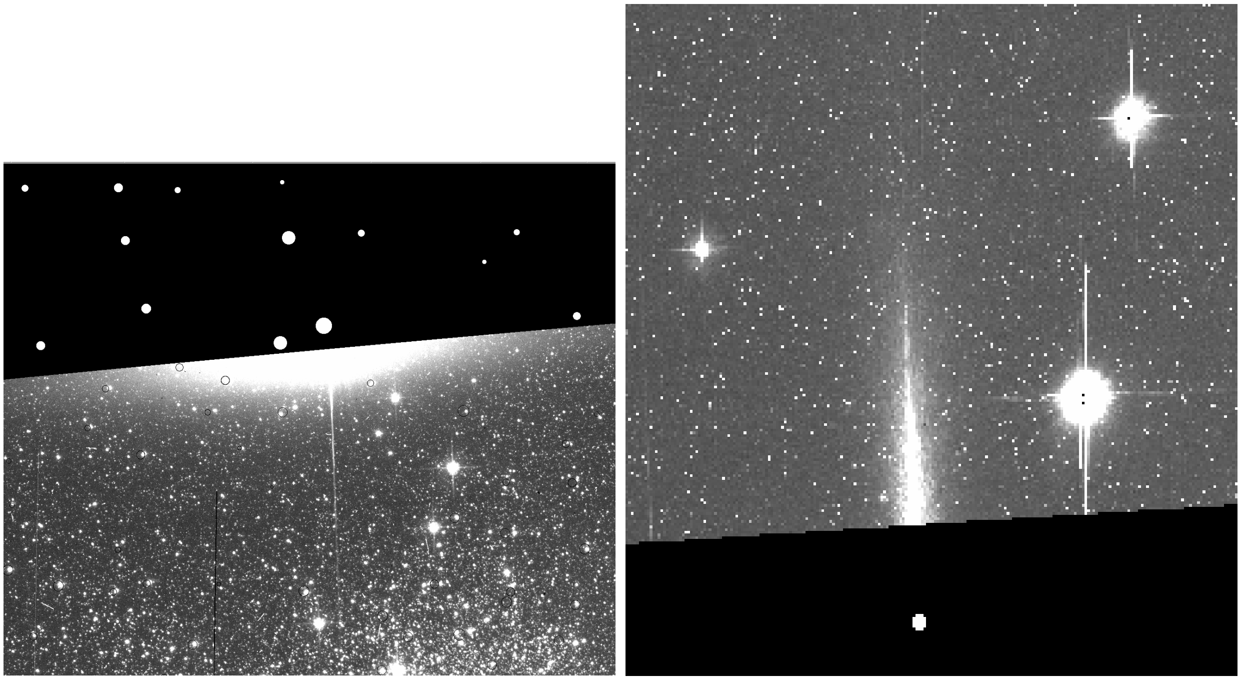

(a) Edge glow (b) Dragon's breath

Figure 1: Examples of edge glow and dragon's breath artifacts in ACS/WFC images. Hubble Guide Star Catalog entries are marked with white circles with sizes encoding magnitudes.

1 Introduction

ACS/WFC images can suffer from a number of optical and scattered light anomalies. Most of the optical anomalies that affect ACS have been well characterized (ACS Data Handbook Section 4.5; ISR 2008-01; Hartig et al. 2002; Hartig 2002). This is not the case for the anomalies known as "dragon's breath" and edge glow (Figure 1). Dragon's breath is caused by light reflections being scattered back to the detector. There is a knife-edged mask in front of the CCD that scatters light back to the detector when its back side is illuminated by reflections from the CCD surface. These phenomena were discovered in early testing of ACS and were mitigated by sharpening the knife edges and coating them black. However, when point sources fall on the edge of the mask, scattering still occurs (Hartig et al. 2002).

Although ACS was designed with a requirement limiting the amount of energy that may be contained in an anomalous feature relative to the object producing it, this scattering exceeds that limit by an order of magnitude (Hartig et al. 2002). These anomalies can have potentially severe effects on data but can be avoided when designing observations.

In this report, we identify the upper right and lower left corners of the detector in (−V2, V3) coordinates[1] as the most severely affected regions of ACS. We quantify the length of the artifacts as a function of stellar magnitude. We also provide interactive webpages showing all identified artifacts to aid the community in preparing their ACS/WFC imaging observations.

[1]The (−V2, V3) coordinate system is the one used for normal ACS image display, where East is 90 deg clockwise of North on the sky.

2 Method

In November 2013, the Mikulski Archive for Space Telescopes (MAST) team provided us (the ACS instrument team) with all full-frame raw ACS/WFC images obtained to date, sorted by HST cycle and anneal date. We visually searched for dragon's breath and edge glow anomalies in all of the F606W and F814W images with exposure times longer than 350 seconds. (2,893 and 5,680 images, respectively, in each filter). We took care (especially in more crowded fields) not to mistake other features such as glint[2] or diffraction spikes for dragon's breath. We also measured the approximate length (in pixels) of each artifact in the F606W images by visual inspection.

For each frame that contained one or more of these anomalies, we created a distortion-corrected FITS image with an overlay of objects from the 2MASS point source catalog[3] (Skrutskie et al. 2006). Using these images (Figure 2), we matched each scattered light anomaly with the "offending star" responsible for it (Figure 3). All dragon's breath and edge glow anomalies include a linear feature that points back to the offending star just outside the ACS/WFC field of view. We recorded the approximate locations (RA, Dec) of these offending stars and then matched them to entries[4] in the Hubble Guide Star Catalog II (GSC II).[5] We used a search radius of $5''$ to allow for small in the global astrometry, and we only retained unambiguous matches (a single match within $5''$). After matching to GSC II stars, our absolute astrometric accuracy improves from a few arcseconds to $\sim 0.1 - 0.3''$.

The guide star catalog includes magnitudes in photographic J and F filters, which are similar to Johnson-Cousins B and R filters with effective wavelengths of ~4400Å and 6700Å, respectively (e.g., Couch et al. 1980). Due to the lack of J magnitude information for many of the stars, we used the F magnitudes in our analyses. We assume the F606W and F814W magnitudes to be both roughly equal to the F magnitude without any color correction. This is accurate to within a few tenths of a magnitude for most stars.

We then normalized the magnitude of each star based on the image exposure time in seconds divided by 500:

$$mag500 = F_{mag} - 2.5\log(\frac{exptime}{500})$$

The resulting $mag500$ is a measure of the total fluence, or flux multiplied by exposure time (divided by 500):

$$flux500 = 10^{-0.4\times mag500} = flux \times (\frac{exptime}{500})$$

The greater the fluence, the more charge deposited onto the CCD, and the greater the scattered light artifact for a given star position relative to the ACS/WFC detectors.

[2]Glint is a rare anomaly produced by bright starlight projected into the chip gap and scattering off residual indium solder (Hartig 2002).

[3]http://tdc-www.harvard.edu/catalogs/tmpsc.html

[4]While most entries in the GSC are stars, a small fraction of these objects are galaxies.

[5]https://archive.stsci.edu/gsc/

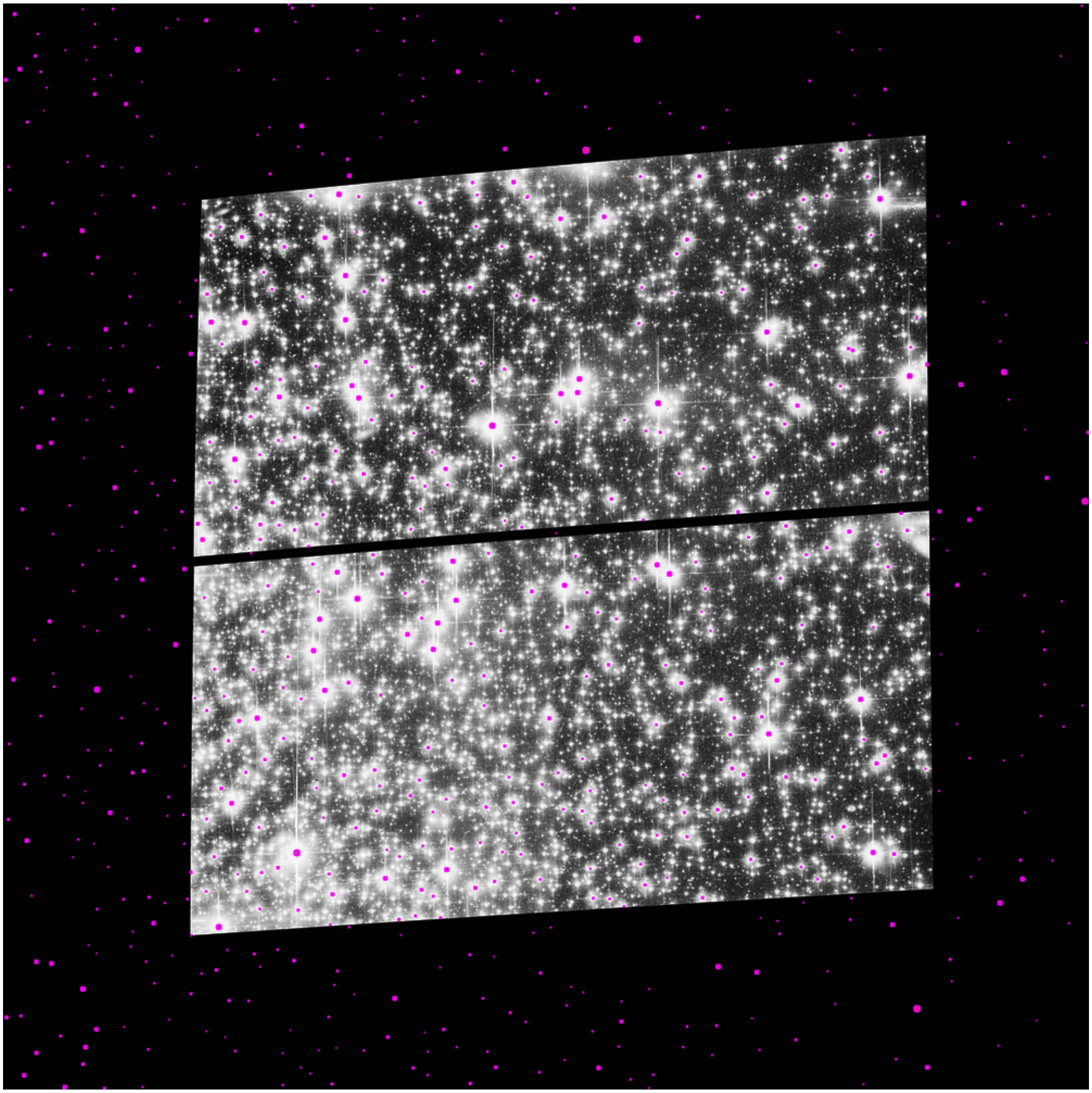

Figure 2: 2MASS stars overlayed on ACS/WFC full frame image. Here the stars are shown as solid magenta circles with sizes corresponding to their brightnesses.

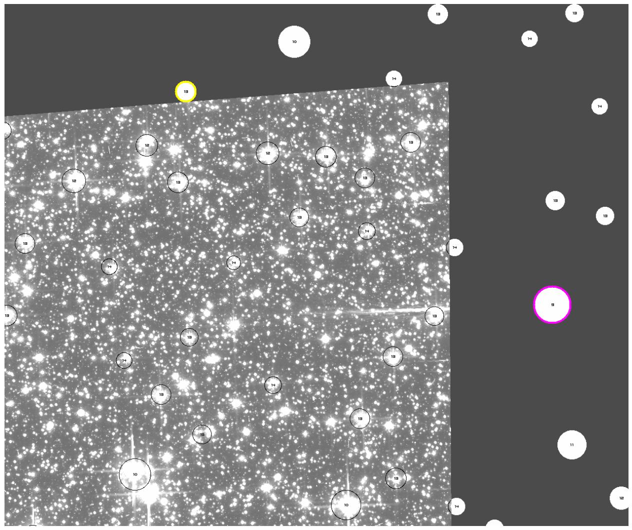

Figure 3: A portion of an ACS/WFC image with the 2MASS overlay in white. The offending star associated with the larger dragon's breath feature is marked in pink. The star marked in yellow is an example of a star on the edge of the chip, which is causing a faint diffraction spike not considered in our analyses.

3 Results

How Dragon's Breath Can Manifest

Through the cataloging process we discovered that dragon's breath can appear in different forms. The name "dragon's breath" comes from classic examples as seen in Figure 4, which look like fire shooting onto the frame. The scattering can also take on more irregular forms as seen in Figure 5.

The size and shape of the anomaly depends on the location of the star relative to the detector. Even relatively small shifts in location (of a few arcseconds) can have significant effects, as we found by inspecting individual stars that caused scattering in multiple dithered exposures. Take the particularly egregious example of a star near the corner of the chip in Figure 6. These two instances of scatter are caused by the same star in slightly different positions (offset by $\sim 3''$) with respect to the detector. Figure 7 shows another instance of corner scattering which changes with the position of the star. This location dependency is not limited to the corners and can occur anywhere around the detector.

We also inspected cases where observations were made in both filters at the same position during the same visit. Figure 8 shows one such example. Small differences in the size and shape of the dragon's breath are apparent. We attribute these differences primarily to the different exposure times in each filter – the image with the greater exposure time has more pronounced dragon's breath.

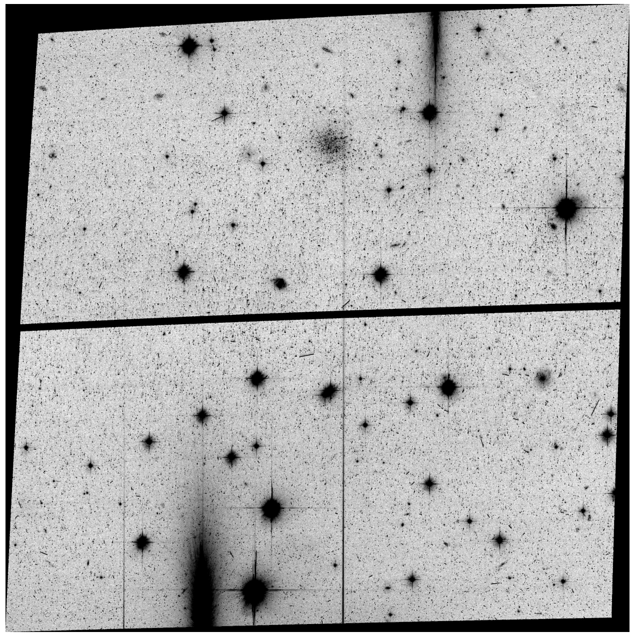

Figure 4: Two cases of classic dragon's breath along the bottom edge (toward the left) and top edge (toward the right) of this image. Unrelated long thin diffraction spikes are also observed. This HST "preview" image was generated by MAST and is available at https://archive.stsci.edu/missions/hst/previews/JBPK/JBPK06H9Q.jpg

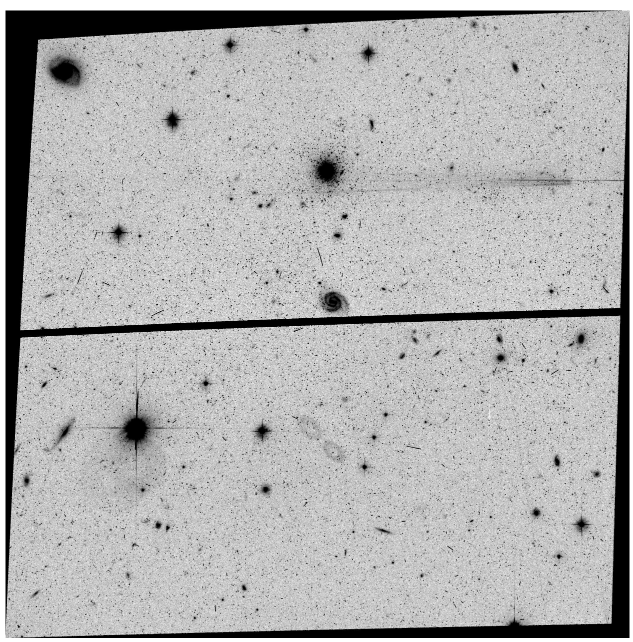

Figure 5: Elongated dragon's breath on the upper right side stretches to the center of the detector. Other artifacts (ghosts and a figure 8) are also observed. This HST MAST preview image is available at https://archive.stsci.edu/missions/hst/previews/J96G/J96G07JXQ.jpg.

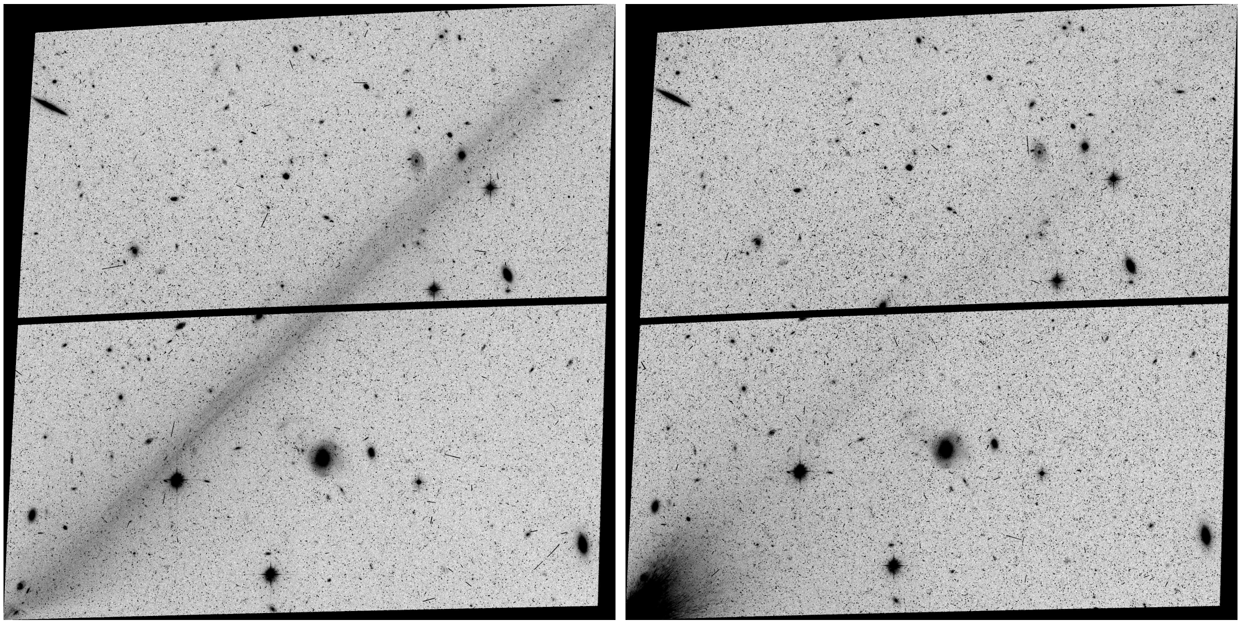

(a) Frame j8de59xwq (b) Frame j8de59y0q

Figure 6: Corner scattering from the same star ($mag500 = 11.3$) just below and to the left of the ACS/WFC field of view for two F606W images slightly offset from one another.

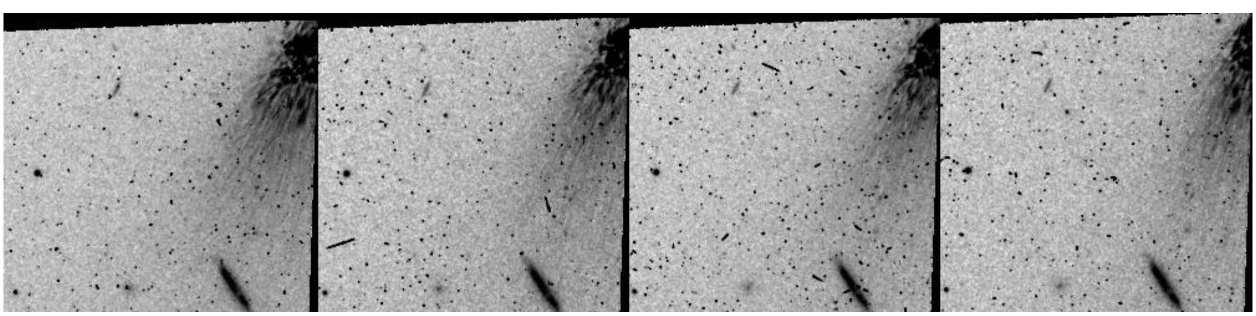

Figure 7: Corner scattering from the same star ($mag500 = 13.2$) in four dithered observations: j8zq07zvq, -zyq, -zwq, and -a1q.

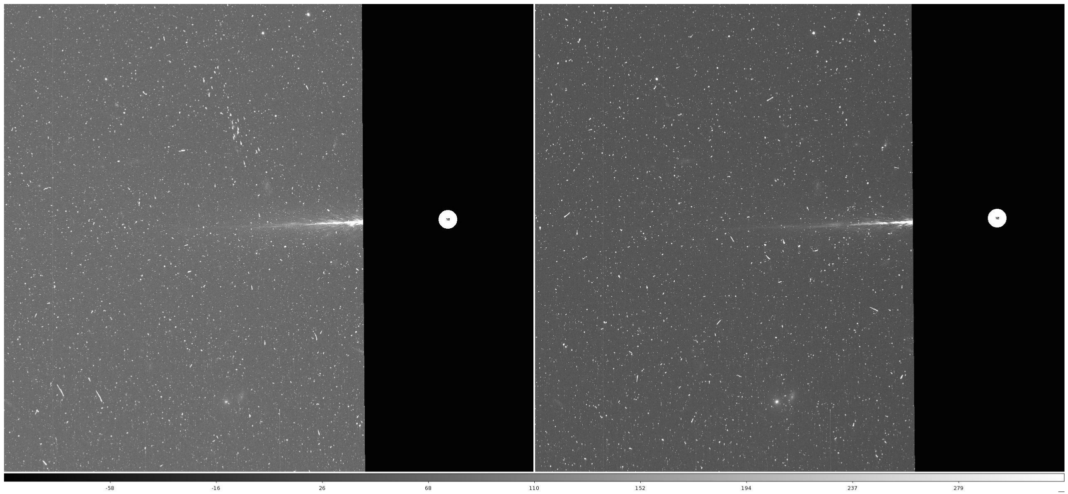

Figure 8: Two observations of the same location on the sky in F606W (left) and F814W (right). The star just to the right of the detector (filled circle) has a photographic F (roughly R-band) magnitude of 15.4. The F606W exposure is longer than the F814W exposure (510 vs. 350 seconds), resulting in a more pronounced dragon's breath.

Anomaly Map

In Figure 9, we plot the locations of all "offending stars" relative to the ACS/WFC detector. In all, we identified 245 stars affecting 589 images in F606W and 172 stars affecting 235 images in F814W (Figure 10). The vast majority of these ($\sim 90\%$) produce dragon's breath effect; the rest produce edge glow. We find that dragon's breath and edge glow are due to stars located in thin regions ($\sim 3''$ wide) just outside the detector field of view, and preferentially near the upper right and lower left corners in ($-$V2, V3) coordinates. Stars causing dragon's breath are $\sim 7'' - 16''$ outside the field of view; stars causing edge glow are generally closer: $\sim 2'' - 4''$ away.

For dragon's breath, we provide the locations of stellar loci in our coordinate system. The offending stars lie along lines $y = mx + b$ with slopes and y-intercepts:

Side	m	b
left	-18	16200
top	0.049	5208
right	-21.42	118000
bottom	0.045	610

These lines are shown in Figure 9. For reference, we also provide the positions of the corners of the ACS/WFC detectors in this 6,000 $\times$ 6,000 pixel coordinate system:

Detector	x	y
WFC1	1035	851
WFC1	5141	1109
WFC1	5118	3198
WFC1	1056	2891
WFC2	1053	2943
WFC2	5115	3253
WFC2	5099	5272
WFC2	1098	4916

This serves as a step toward providing "avoidance zones" to users. Bright stars placed near these lines may yield artifacts. The magnitude of the artifact depends in part on the magnitude of the star.

Magnitudes

The GSC II contains stars (and some galaxies) down to 20th magnitude. All the offending stars have magnitudes. Only two of these stars are fainter than 18th magnitude (Figure 11). Stars brighter than 10th magnitude would presumably cause artifacts as well, but these are more rare, and none landed on the anomaly loci in the images we studied.

Stars which deposit more light onto the detector over the duration of the exposure generally produce larger artifacts, as we show quantitatively in Figure 12. We plot the lengths (in pixels) of the artifacts versus the normalized magnitudes $mag500$ of the stars which produced them. Consider stars located in the anomaly loci just outside the detector field of view in a 500-second exposure. A 10th magnitude star will typically produce an artifact about 1,000 pixels long (about 1/4 the length of the ACS detectors). At the faint end, an 18th magnitude star will typically produce an artifact only about 100 pixels long. But there is significant scatter in this correlation depending on the position of the star relative to the detectors. For example, in frame j8de59xwq, a star with photographic F magnitude 11.7 just off the corner of the detector produces our largest observed artifact: 6,000 pixels long, stretching all the way across the ACS field of view diagonally from one corner to the other (Figure 6a). In this 720-second exposure, the stellar normalized magnitude $mag500 = 11.7 - 2.5\log(720/500) = 11.3$.

4 Web Interface

We used Bokeh[6] to create two interactive webpage plots that allow users to explore our results. The first plot available online[7] (screenshot shown in Figure 13) is similar in appearance to the anomaly map in Figure 9. Each point represents a star near an ACS/WFC observation, and the black lines represent the ACS/WFC chips. Users can hover over the location of each offending star and see the corresponding image containing a scattered light anomaly. Above the image we report information including the guide star name, the name

[6]http://bokeh.pydata.org

[7]http://www.stsci.edu/hst/acs/performance/anomalies

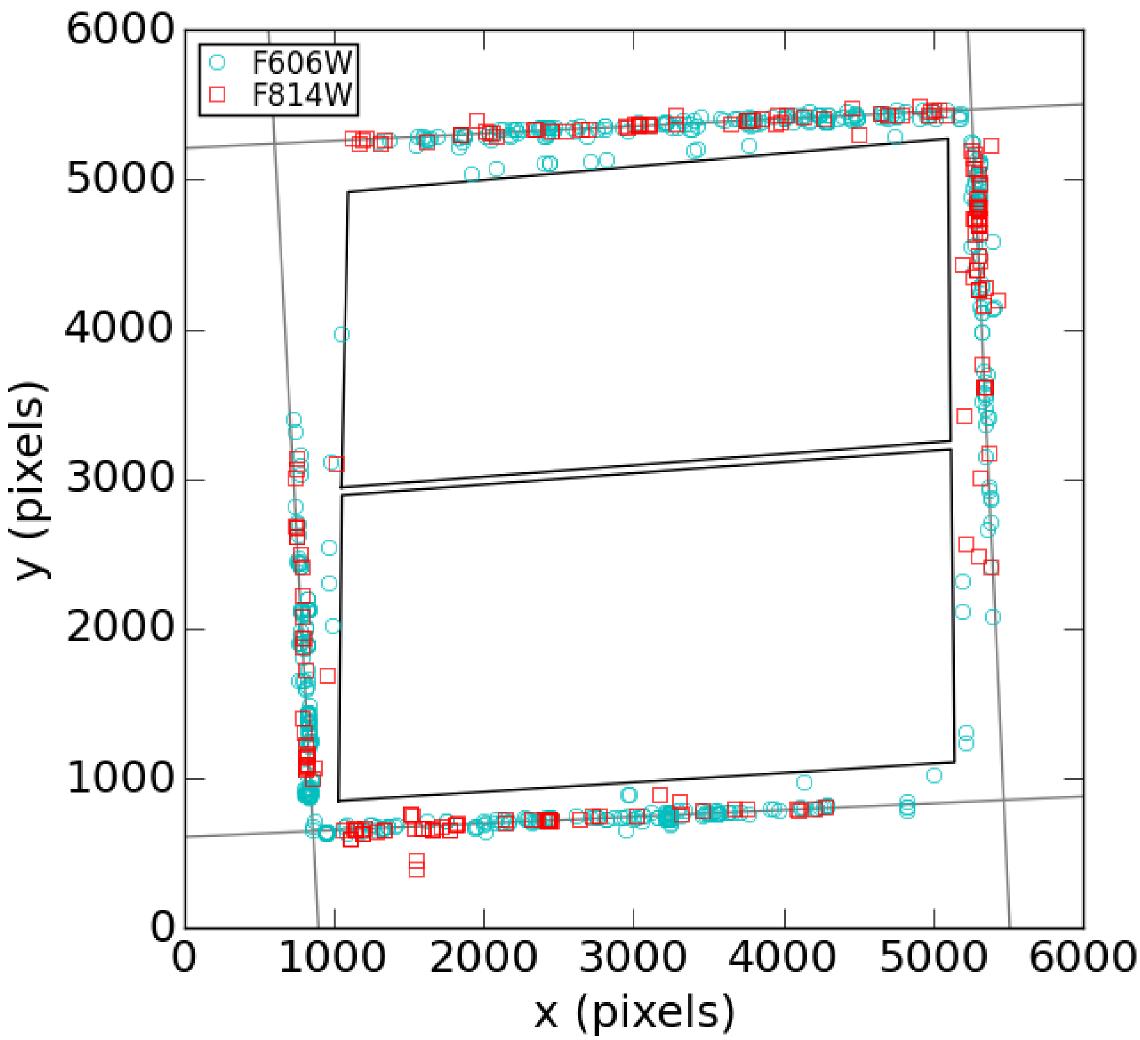

Figure 9: Positions relative to the ACS/WFC detectors (black trapezoids) of stars (cyan circles and red squares) that caused dragon's breath or edge glow scattered light artifacts in F606W and F814W images. Axes are in units of distortion-corrected pixels 0.05″ on a side. In HST coordinates: V3 is up and V2 is left. The full frame is 6,000 × 6,000 pixels, centered on the ACS/WFC detectors. Gray lines show straight-line fits to the positions of the offending stars with formulae given in the text.

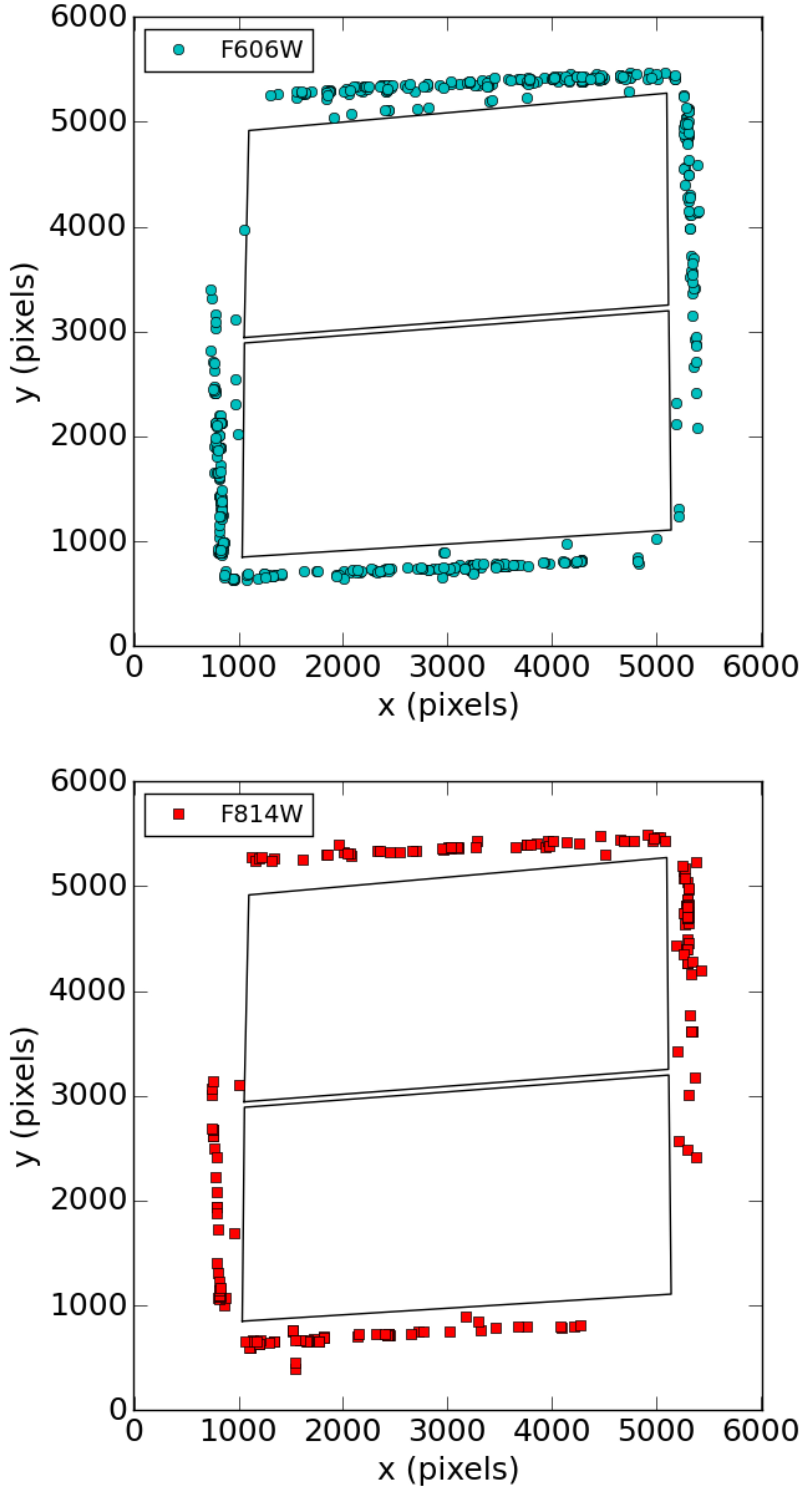

Figure 10: Positions relative to the ACS/WFC detectors of stars that caused dragon's breath or edge glow scattered light artifacts, as in Figure 9 but plotted separately for F606W images (top) and F814W images (bottom).

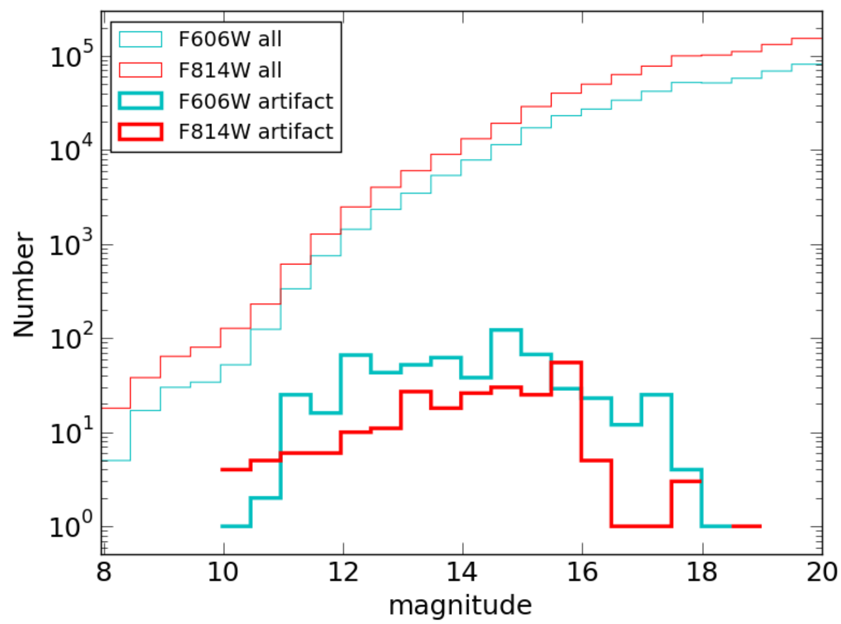

Figure 11: Histograms of photographic F magnitudes (roughly R-band) of all GSC II stars within 3′ of the ACS images we studied (thin lines) and that of the "offending stars" producing dragon's breath and edge glow anomalies (thick lines).

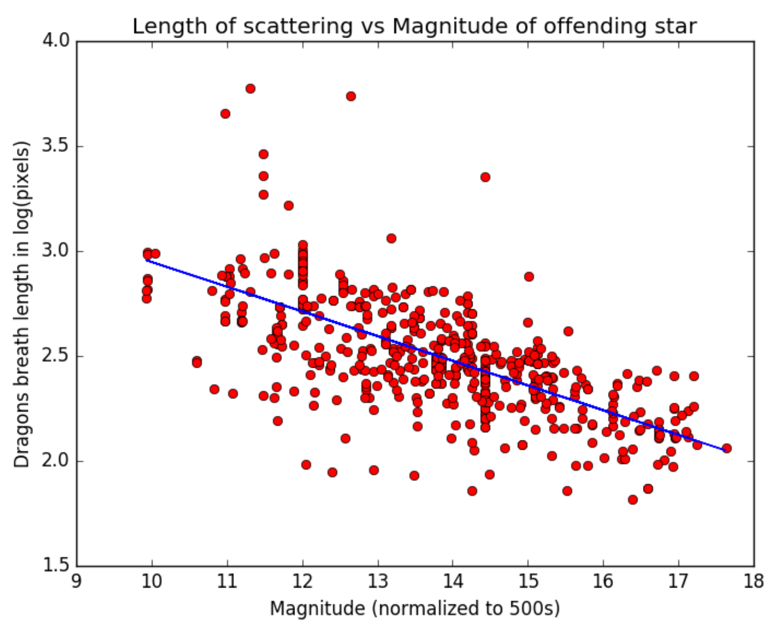

Figure 12: Measured length of dragon's breath and edge glow artifacts (in pixels) in F606W images versus the normalized magnitude $mag500$ of stars that produced them.

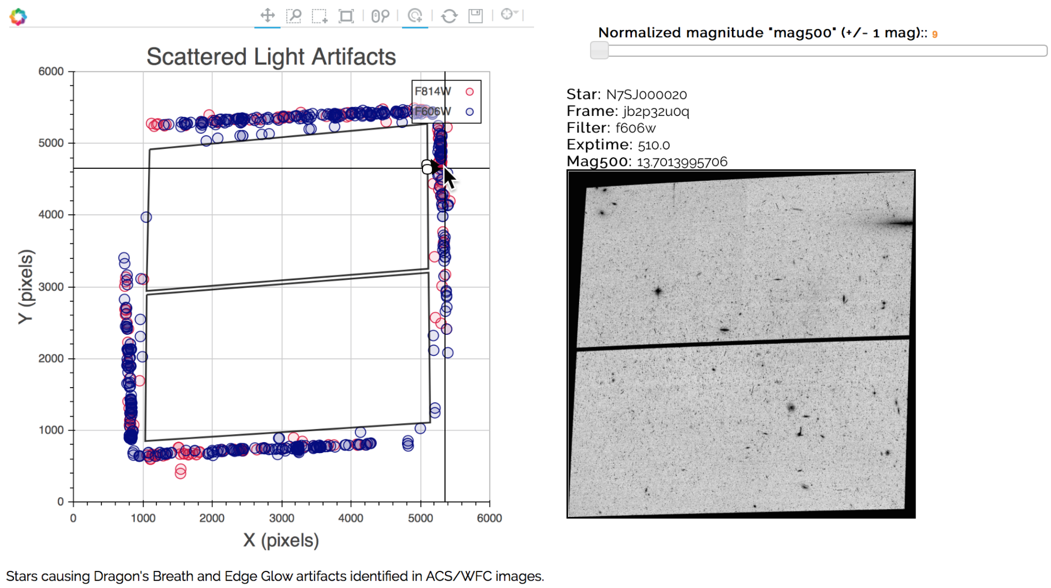

Figure 13: Screenshot of an interactive webpage showing all anomalies cataloged in this work. In the plot on the left, blue and red points represent stars just outside the ACS field of view for F606W and F814W observations, respectively. Hovering over each point reveals the ACS image near that star (in the right panel), including the dragon's breath or edge glow artifact(s). The webpage is available at http://www.stsci.edu/hst/acs/performance/anomalies.

of the image, the filter used, the exposure time, and $mag500$. By default, the plot displays the location of all offending stars. There is also a slider that allows the user to select stars in a range $mag500 \pm 1$. Users may also pan and zoom into the plot.

The second plot available online (screenshot shown in Figure 14) shows all the brightest GSC II stars ($9 \lesssim mag500 \lesssim 13$) within $3'$ of the ACS images we studied. These include stars at a broader range of positions, including many within the ACS/WFC field of view, to show the impact such stars have on observations.

We have found these tools useful for exploring the correlation of $mag500$ with the severity of the artifacts, as well as examples of scattered light appearing in multiple dithered observations and in multiple filters. For example, in Figure 15 we show an example of two dithered F606W images with similar exposure times and pointings offset from one another by a few arcseconds. One of the images shows a significant dragon's breath anomaly, but the other shows much fainter dragon's breath.

5 Conclusions

In ACS/WFC images, dragon's breath and edge glow scattered light artifacts are caused by stars located in narrow regions just outside the field of view (Figure 9). Small positional shifts ($\sim$1 arcsecond) can significantly affect the size and shape of the artifacts. For a given position, the amplitude of the artifact depends on the total charge deposited — a function of the stellar magnitude and the image exposure time, but not the choice of filter. On average,

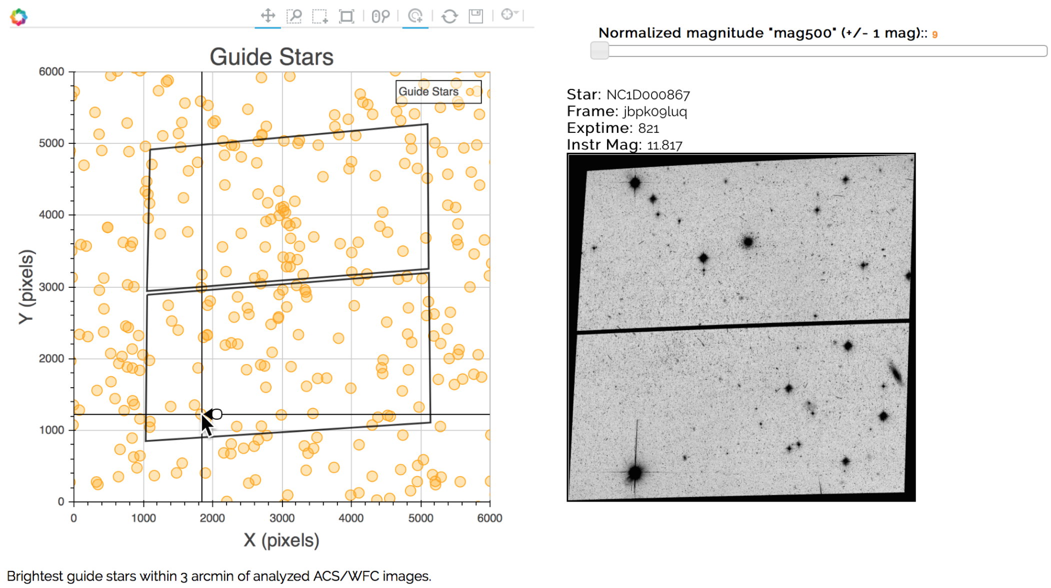

Figure 14: Screenshot of an interactive webpage showing the brightest guide stars ($9 \lesssim mag500 \lesssim 13$) within $3'$ of the ACS images studied. Each yellow point represents a star. Hovering over each point reveals the ACS image of (or near) that star. http://www.stsci.edu/hst/acs/performance/anomalies.

10th magnitude stars produce dragon's breath extending about 1,000 pixels in length, and 18th magnitude stars produce smaller artifacts about 100 pixels long (Figure 12). Much larger artifacts have also been observed, spanning diagonally across the full field of view (6,000 pixels).

Images of all the artifacts we identified are available online via interactive plot webpages. These tools may help users plan their ACS/WFC imaging observations near bright stars. Users may see examples of artifacts due to stars of a given magnitude at a given position relative to the ACS/WFC field of view. ACS/WFC imaging observations should be designed to avoid positioning relatively bright stars in the anomaly loci (Figure 9). Fainter stars are less of a concern, producing smaller artifacts similar to the diffraction spikes observed around many stars.

6 Acknowledgments

We thank Ralph Bohlin, Andrea Bellini, and Jenna Ryon for useful comments. The Space Telescope Science Institute (STScI) is operated by the Association of Universities for Research in Astronomy, Inc. (AURA) under NASA contract NAS 5-26555. ACS was developed under NASA contract NAS 5-32864. We obtained images from the Mikulski Archive for Space Telescopes (MAST).

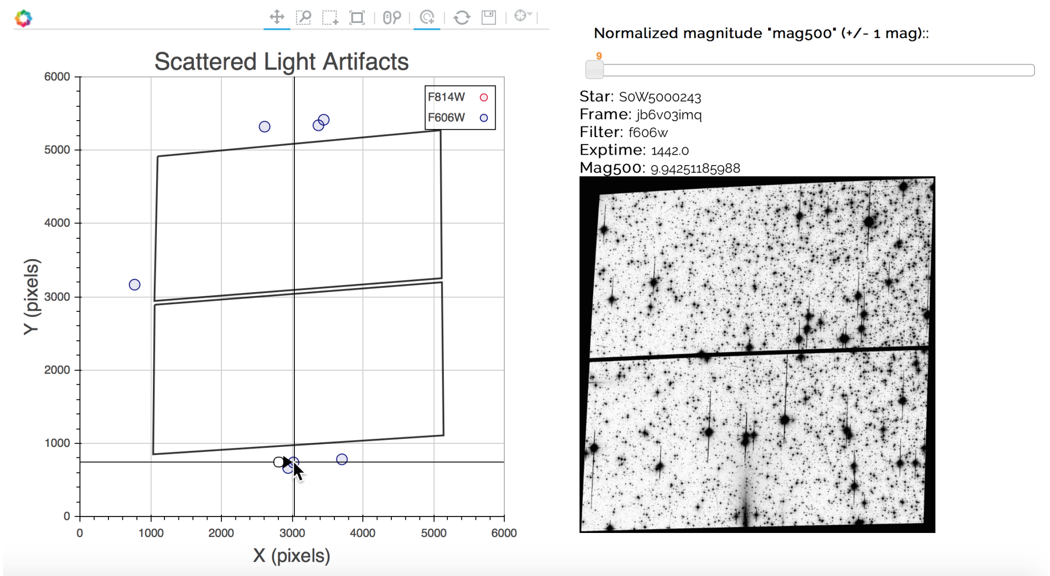

(a) Bright dragon's breath

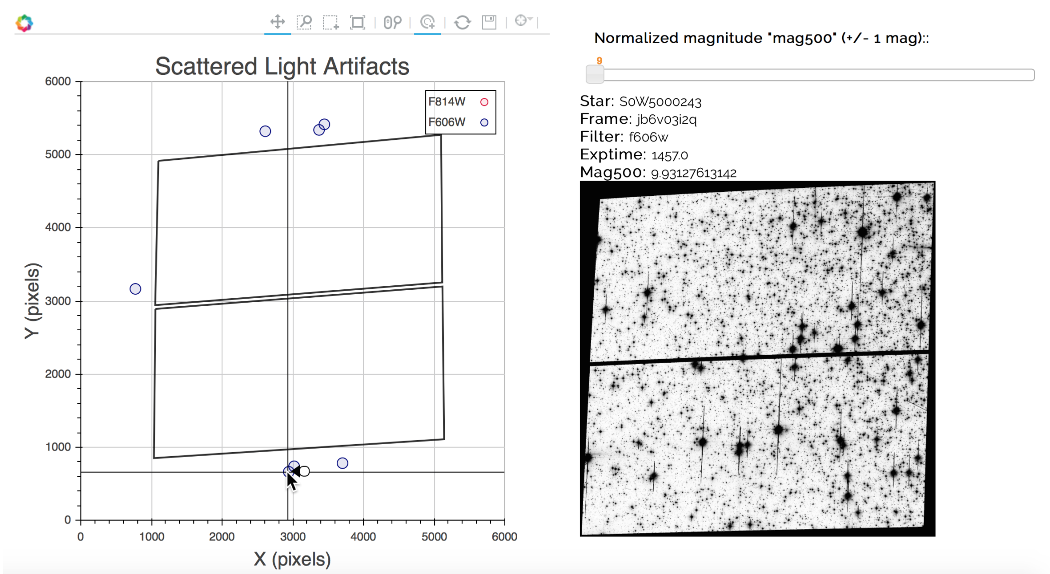

(b) Faint dragon's breath

Figure 15: Two F606W imaging observations with similar exposure times, slightly offset from one another (by a few arcseconds), both near a 10th magnitude star (just below the field of view). The top image shows a significant dragon's breath anomaly about 1,000 pixels long. The bottom image shows much fainter scattered light extending about 600 pixels in length (but much narrower).

7 References

ACS Image Anomalies: http://www.stsci.edu/hst/acs/performance/anomalies

ACS Instrument Science Reports (ISRs): http://www.stsci.edu/hst/acs/documents/isrs

Couch, W. J. et al. 1980, PASP, 92, 746, "A Photometric System for Limiting jf Photography - Part One - the Primary Standards"

Hartig, G. F. et al. 2002, "On-orbit alignment and imaging performance of the HST Advanced Camera for Surveys"
http://www.stsci.edu/hst/acs/performance/anomalies/ACS_ghosts.pdf

Hartig, G. F. 2002, "Scatter from the ACS WFC Inter-chip Gap"
http://www.stsci.edu/hst/acs/performance/anomalies/ACS_scatter.pdf

Lucas, R. et al. 2016, ACS Data Handbook v8.0
http://www.stsci.edu/hst/acs/documents/handbooks/currentDHB

Skrutskie, M. F. et al. 2006, AJ, 131, 1163, "The Two Micron All Sky Survey (2MASS)"

Stankiewicz, M. et al. 2008, "ACS CCD Image Anomalies in the Hubble Legacy Archive" (HLA ISR 08-01)
http://www.stsci.edu/hst/acs/documents/isrs/hlaisr0801.pdf